Malaysian Simulation SOCIETY
http://amsjournal.ams-mss.org
APPLICATIONS OF MODELLING AND SIMULATION
eISSN 2600-8084
VOL 2, NO. 3, 2018, 107-113

Modelling and PID Control of an In-Wheel Motor

Muhammad I. Faruk[1*], Shehu S. Farinwata[2] and Auwalu M. Abdullahi[3]

[1]Department of Physics and Electronics Bayero University Kano, Nigeria.
[2]Department of Mechatronics and System Engineering, Abubakar Tafawa Balewa University Bauchi, Nigeria.
[3]Department of Mechatronics Engineering, Bayero University Kano, Nigeria.

[*]Corresponding author: ifmuhammad.phy@buk.edu.ng

Submitted 11 October 2018, Revised 10 November 2018, Accepted 14 November 2018.

Abstract: In-wheel motor (IWM) is a complex non-linear and multi-changeable control system. The non-linear magnetic characteristics of the motor under normally saturated operation and other internal parameter value variations with the environment makes their control and optimisation relatively complex. A suitable control algorithm often has to be employed in other to achieve the required performance and other control objectives. In this work, the dynamic model of the IWM using hard modelling is presented. The controllability and observability of the model are also verified. Simulation using Matlab Simulink is used to validate the model and subsequently developing a classical proportional-integral-derivative (PID) controller for the system. The simulation results shows that the PID controller provides satisfactory trajectory tracking of the reference signal.

Keywords: Dynamic model; In-wheel motor; Modelling; PID.

1. INTRODUCTION

Optimising and conserving energy is a large focus of society today. This is largely due to a predicted energy shortage if global consumption continues on its current trajectory [1]. Many ways of saving energy therefore, have been researched and implemented to this point, such as super-efficient windows for large buildings, lights bulbs that use minimal electricity, as well as smarter manufacturing technologies such as optimising blast furnace operation [2]. Some of the most significant efforts in energy saving, however, has been put into the area of industrial and personal transportation. The large majority of vehicles still run on fossil fuels, but an increasing amount of research has been put into developing and optimising alternative energy sources such as electric, biofuels, natural gas and even solar power for transportation. Hybrid vehicles attempt to mate the utility of a gasoline/diesel engine with the environmentally friendly characteristics of an electric drive. In order to push the envelope of sustainability even further, however, an increasing effort has been put into developing vehicles that run on pure electric power (i.e. electric motors) [3].

In-wheel motor (IWM) is an electric motor that is incorporated into the center of a wheel and drives it directly. These wheels contain not only the braking components, but also all of the functionality that was formerly performed by the engine, transmission, clutch, suspension and other related parts. The motor is installed close to the drive wheel and moves the wheel through extremely small drive shaft. The motor apply torque directly to the wheel and it is only linked via electrical connections that converge to a central controller hub. Such a configuration results in over-actuation (which causes instability in driving around corners or even in a straight line) and thus results in more optimisation potential. With this enhanced capability, however, a significant amount of complexity and complicated control problems are also inevitably introduced. If a suitable control strategy can be developed, though, the capacity for savings is vast, as there are no losses due to mechanical energy transfer, as well as the capability of each wheel to be controlled independently for maximum efficiency. Much of the control effort up to this point has been put towards the area of safety and stability of such motors. Therefore, various control strategies such as road-friction estimation [4], a system of electric differentials [5], as well as motion tracking control schemes [6] have been investigated in order to provide a comprehensive mechanism for accurately driving the IWM. The IWM presented in this paper is a permanent-magnet brushless direct-current (BLDC) electric motor as used in [7-8,18].

2. SURVEY OF PERTINENT LITERATURE

There were many proposed methods for IWM control and optimisation given in various literature, ranging from classical [9], intelligent and adaptive techniques [10]. In a more recent and related work [11], the way in which, constituent interrelated parts were arranged and operation principle of the magnetic-geared PM motor were presented. Stator structure optimisation was employed to improve the motor performance and also presented an alternative operation condition with the modulation layer rotating. The procedure proved effective and further verified with finite element analysis. The result shows a rational

reduction in the rotor speed and increase the output torque giving the motor distinct advantages as a potential candidate for low-speed and high-toque direct drive applications. However the method presented pose certain setbacks, relative to high torque ripple due to the fringing effect in the slots of the modulation layer and stator. Also finite element method is still improving and rely heavily on numerical integration. It is also time demanding in relation to programming making it difficult for prototype implementation and verification.

Liang et al. [12] presented an analytical predictive model for a spoke type permanent magnet IWM. The motor was divided into six sub-domains based on the boundary conditions which were marched by simplifying the magnet into sector magnets. Then their dimensions were calculated using the lumped magnetic circuit model. The process of which gave rise to the ability to calculate the motor properties (back EMF, torque) using Poisson's and Laplace transformation. Thereafter, the result of which was verified using finite element method, shows the accuracy of the model. Farinwata and Vachtsevanos [13] presented a theory which provides a systematic frame work for analysing the robustness of fuzzy idle speed controller for linear and non-linear systems on a nominal plant. Small bounded parameter uncertainty and external disturbances were considered. The method selected an appropriate performance measure as a Lyapunov like function of the nominal plant and used to minimise the error sensitivity. Also the robustness was analysed by observing the definiteness condition of a simple matrix. Zero crossing point detection of back EMF was presented in [14] on a brushless DC motor using a high speed microcontroller for system optimisation. The technique presented proved efficient though suffers a slow response and requires high level of expertise in development and implementation. In [15], some control strategies for a complex multivariable nonlinear system (brushless DC motor) were proposed. The paper presented a conventional control strategy and an advanced control algorithm implemented on a transfer function model represented system. Their findings were compared and contrasted, and the implementation of these algorithms revealed the most effective algorithm. However, for a complex multivariable system employing such an approach is susceptible to errors because several calculations were involved.

In another related literature, a flexible power demand architecture was presented which gave flexibility to the driveline and more utilisation of the IWM of the hybrid electric vehicles so as to achieve better fuel economy [16]. Firstly, the trajectory of power demand was obtained, then an optimal base line trajectory was formulated. The formulated base line trajectory was thereby solved using Pontryagin's minimum principle. The method showed a promising level of improved fuel economy. On the other hand, the technique was not economically cost friendly in terms of implementation due to the fact that technical provisions has to be provided for both the internal combustion engine unit as well as that of the IWM.

3. METHODOLOGY

3.1 Electrical Model of the Circuit

Considering the circuit of the system as shown in Figure 1, hard modeling is employed (i.e. using scientific principles; Newton's law, Kirchhoff's law, thermodynamic laws) to derive the system dynamic model. Using $F = ma$, the torque equations are given by

$$T = I_L \dot{w}(t) \tag{1}$$

$$T = K_T i(t) \tag{2}$$

$$V_B = K_B w(t) \tag{3}$$

By applying the Kirchhoff's Voltage Law,

$$V_{(s)} = Ri(t) + L\frac{di(t)}{dt} + V_B \tag{4}$$

The two torque equations (Equations (1) and (2)) are considered to yield a single equation that will relate the current I to the change in angular velocity, $\dot{w}(t)$. Therefore the torque T in now given by

$$K_T i(t) = I_L \dot{w}(t) \tag{5}$$

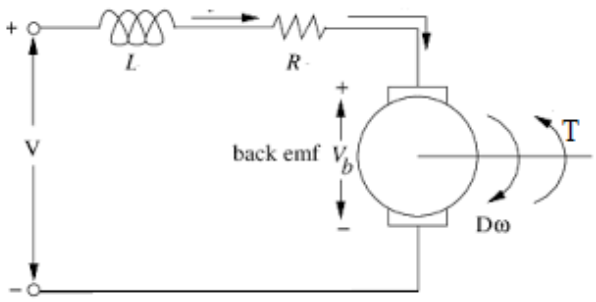

Figure 1. Electric motor circuit diagram

Substituting Equation (3) into Equation (4) to obtain the second differential equation relating the back EMF, inductance and the resistance yields $V_{(s)} = Ri(t) + L\frac{di(t)}{dt} + K_B w(t)$.

The two differential equations representing the dynamics of the IWM system can be written as

$$\frac{dw(t)}{dt} = \frac{K_T}{I_L} i(t) \tag{6}$$

$$\frac{di(t)}{dt} = \frac{1}{L}\left[V_{(s)} - Ri(t) - K_B w(t)\right] \tag{7}$$

where:

R – Motor resistance, L – Motor inductance,
T - Torque, I_L - Moment of inertia of the load
w - Angular velocity, $\dot{w}(t)$ - Acceleration
K_T - Torque constant, K_B - Back EMF constant

Thereafter a numerical solution of the set of differential equation is used to model the system behaviour in time using Matlab Simulink. The process of integration lies at the core of the simulation and hence the integrator blocks forms the central basis of the simulation block diagram. Each state variable requires an integrator block and, the initial conditions for each state variable were set within the block diagram. The outputs of the integrators are the state variables themselves. These outputs are then used to build the derivatives (inputs to each integrator). Hence, in order to simulate the system dynamics, Equations (6) and (7) are integrated assuming zero initial conditions to yield:

$$w(t) = \int \frac{K_T}{I_L} i(t) \tag{8}$$

$$i(t) = \int \frac{1}{L}\left[V_{(s)} - Ri(t) - K_B w(t)\right] \tag{9}$$

The process was completed by generating the system block diagram as in Figure 2 using Equations (8) and (9). Table 1 shows the system parameters used in this simulation work. The model parameters as well as the initial conditions were then specified, thereafter selecting an arbitrary input to excite the system so as to study the response of the system to inputs and initial conditions. Through this development, the system transfer function was obtained as

$$TF = \frac{20}{s^2 + 5s + 4.4} \tag{10}$$

3.2 Controllability and Observability

3.2.1 System State Space Model

The IWM state space representation was also obtained using Simulink as in Equation (11), in order to verify the system controllability and observability using the existing theorem. These theoretical verifications are independent of the controller design, rather performed merely for system observation.

Table 1. System Parameters

Parameters	K_T (Nm)	K_B (vrad^{-1})	I_L (kgm^{-3})	L (H)	R (Ω)
Value	0.02	0.22	0.005	0.2	1

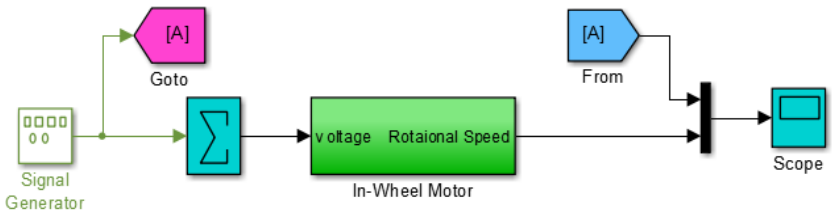

Figure 2. Model Simulink block diagram

$$\dot{X} = \begin{bmatrix} 0 & 4 \\ -1.1 & -5 \end{bmatrix} x(t) + \begin{bmatrix} 0 \\ 5 \end{bmatrix} u(t) \quad (11)$$

$$y = [1 \quad 0]\, x(t)$$

Where x is a state vector, $\dot{X}$ is the derivative of state vector, y is the output vector and u is an input vector

3.2.2 Controllability

Consider the n-dimensional p-input LTI state equation.

$$\dot{X} = Ax(t) + Bu(t), \qquad x \in R^n; u \in R^p \quad (12)$$

where A is an $(n \times n)$ constant system matrix, B is an $(n \times p)$ constant input matrix.

Theorem 1: The theorem states that the n-dimensional (A, B) is Controllable if the $(n \times p)$ controllability matrix $G^C = [B\ AB\ A^2B \ldots \ldots \ldots A^{n-1}B]$ has a rank n (full row rank) [17]. Therefore using the theorem the controllability of the system is verified. The system is found to be controllable, as the matrix is non-singular with full row rank of 2 shown in Equation (13).

$$G^C = \begin{bmatrix} 0 & 20 \\ 5 & -25 \end{bmatrix} \quad (13)$$

The determinant of Equation (13) was computed and found it to be a non-zero determinant hence satisfying the Theorem 1.

3.2.3 Observability

Consider the n-dimensional p-input state equation

$$\dot{X} = Ax(t) + Bu(t) \text{ and } y = Cx(t) + Du(t) \quad (14)$$

where A, B, C and D are respectively $(n \times n)$, $(n \times p)$, $(q \times n)$ and $(q \times p)$ constant matrices.

Theorem 2: States that the n dimensional pair (A, C) is observable if $(nq \times n)$ observability matrix $G^C = [C \quad CA \quad \ldots \quad CA^{n-1}]^T$, has rank n (full column rank) [17]. Also using Theorem 2, the observability of the system is verified. Equation (15) shows that the system is observable because it is non-singular with full column rank of 2.

$$G^O = \begin{bmatrix} 1 & 0 \\ 0 & 4 \end{bmatrix} \quad (15)$$

The system is therefore found to be controllable and observable, since its determinant was found to be non-zero.

4. CONTROLLER DESIGN

The proportional-integral-derivative (PID) controller consists of the combination of proportional (K_p), integral (K_i) and derivative (K_d) control action. The mathematical representation of which is presented in Equation (16).

$$u(t) = K_p e(t) + \frac{K_p}{T_i} \int_0^t e(t)dt + K_p T_d + \frac{de(t)}{dt} \quad (16)$$

The proportional controller is amplifier with an adjustable gain. It reduces the rise time but does not eliminate steady state error. While an integral controller eliminates steady state error for constant or step input but may make the transient response slower. On the other hand, the derivative controller will increase the stability of the system, reduce the overshoot and improve the transient response. The PID controller for the IWM was designed and parameters tuned with reference to the derived system transfer function as in Equation (10) using Matlab Simulink interface.

The block diagram of the controller is presented in Figure 3. $R(s)$ is the input voltage (reference), $E(s)$ is the error signal, $U(s)$ is the output of the controller which becomes input to the IWM, $G(s)$ is the system/plant and $C(s)$ is the system output (speed). In addition, K_p is the proportional gain, T_i is the integral time, and T_d is the derivative time. Having fulfilled the necessary design requirements, the next important objective is tuning of the PID parameters in order to achieve the three major goals i.e. fast response, minimal overshoot and zero steady state error. Manual tuning process was used throughout the design. Figure 4 and Figure 5 show the performance of the system before tuning the controller parameters using step and square wave inputs respectively.

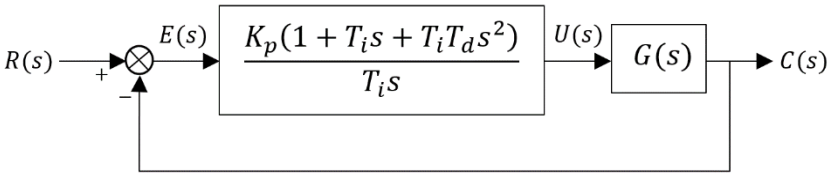

Figure 3. Controller block diagram

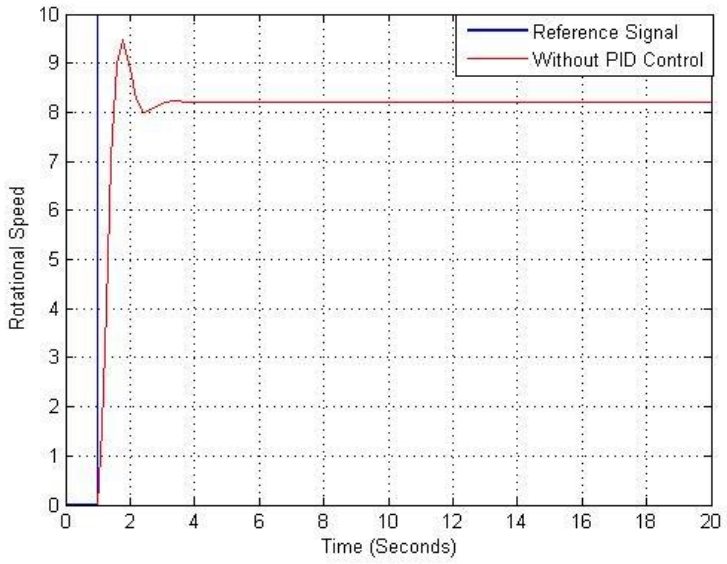

Figure 4. Step response of the IWM model without PID controller

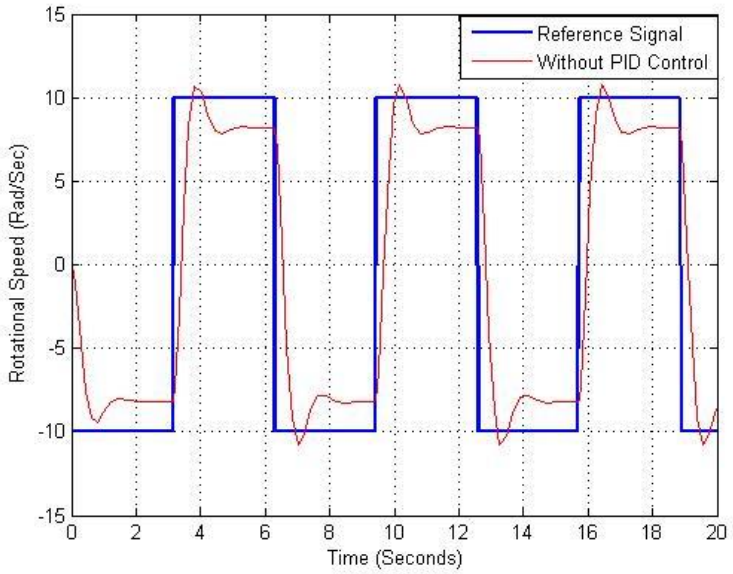

Figure 5. Square-wave input response without PID control

Having obtained the system responses in Figures 4 and 5 using the two different excitation inputs, it can be observed that there is relatively no tracking and at the same time having quite a large steady state error, then tuning the K_p, K_i and K_d parameters preceded. Since the K_p reduces the rise time, increases the overshoot and reduces the steady-state error, the value of which was selected at random until realising a reasonable output. Also the integral control K_i tends to decrease the rise time, increase both the overshoot and the settling time, and reduces the steady-state error, its value was also randomly selected so as to achieve the three aforementioned objectives. The same procedure was applied on the addition of derivative control which tends to reduce both the overshoot and the settling time. The final gains of the classical PID parameters were deduced as K_p = 0.43, K_i = 0.47 and K_d = 0.03.

5. RESULTS AND DISCUSSION

Figure 6 shows the output response performance of the model with PID controller using a step input. It can be seen that the PID controller controls the system to follow the reference input. It can be further observed that the system started smoothly with a better level of consistency in terms of tracking the reference input as compared to the response in Figure 4. Furthermore, the controlled system was able to achieve zero steady state error with minimal overshoot.

Similarly, Figure 7 displays the system performance with PID control using a pulse input signal. It can be observed in Figure 7 that the output response effectively traced the reference signal, in which it completely eliminated the error in the negative half axis of the square wave (i.e. 0-3 s), and then gradually eliminating the overshoot at the positive axis of the square wave (i.e. 4-6 s) when compared with Figure 5. Figure 7 further confirmed that the system achieves stability in the sense that it continued to track the reference signal effectively with zero steady state error.

With the aforementioned development in the rotational speed performance as in Figures 6 and 7, it can be ascertained that a desired speed of response, minimal overshoot and zero steady state error were successfully attained. Table 2 further shows the transient response analysis based on the control measure parameters, where it can be observed that there was an increased efficiency with respect to the values of rise time, peak time, settling time and stability.

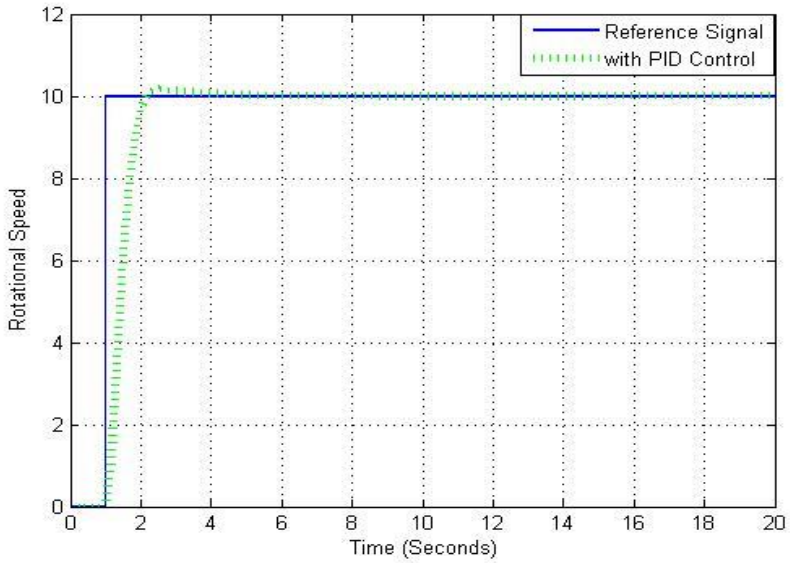

Figure 6. Step response of the IWM with PID

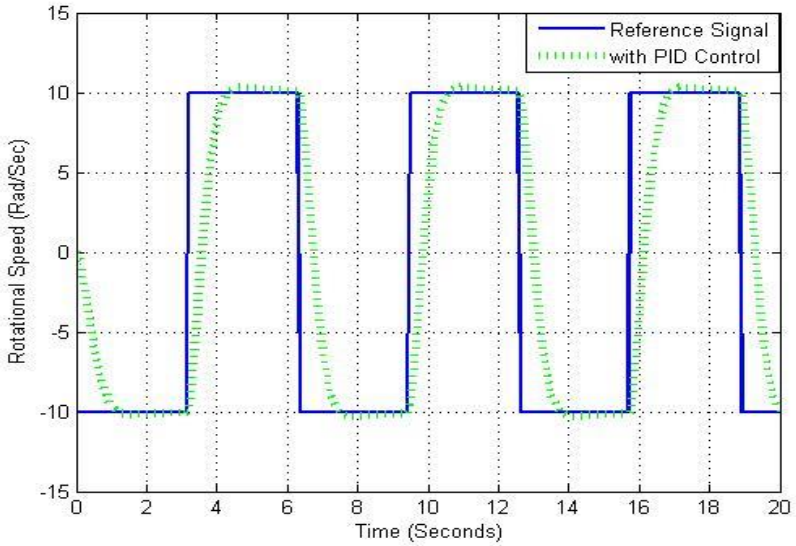

Figure 7. Square-wave response of the IWM using PID control

Table 2. System performances

Control Measure	Without PID Control	PID Control
Rise Time (T_r)	1.09 s	0.71 s
Peak Time (T_p)	4.51 s	1.02 s
Settling Time (T_s)	5.84 s	1.07 s
Overshoot ($\%O_s$)	15.00 %	1.91 %

6. CONCLUSION

The dynamic model of the IWM was obtained and successfully optimised using the PID controller in Matlab Simulink interface. The output responses of both step and square-wave input references shows a highly improved stable system performance. The PID control implemented system can be shown to perform significantly better, than the system without PID control as it was able to improve the IWM startup performance, eliminate offset error, provided a faster time response and most importantly achieved stability. However, the performance can be further improved with more tuning and using more advanced control algorithms.

REFERENCES

[1] Energy overview: Fossil fuels, Institute for Energy Research (Website). http://www.instituteforenergyresearch.org/ (accessed 28.03.14).

[2] Optimizing blast furnace operation to increase efficiency and lower costs, U.S department of energy (Website). http://www.energy.gov/site/prod/file. (accessed 10.03.16).

[3] C. C. Chan and K. T. Chau, *Modern Electric Vehicle Technology*. Oxford, UK: Oxford University Press, 2001.

[4] Y. Chen and J. Wang, Adaptive vehicle speed control with input injections for longitudinal motion independent road frictional condition estimation, *IEEE Transactions on Vehicular Technology*, 60(3), 839–848, 2011.

[5] Y. Chen and J. Wang, Design and evaluation on electric differentials for overactuated electric ground vehicles with four independent in-wheel motors, *IEEE Transactions on Vehicular Technology*, 61(4), 1534–1542, 2012.

[6] Y. Chen and J. Wang, Adaptive energy-efficient control allocation for planar motion control of over-actuated electric ground vehicles, *IEEE Transactions on Control Systems Technology*, 22(4), 1362–1373, 2014.

[7] E. Esmailzadeh , G. R. Vossoughi and A. Goodarzi, Dynamic modeling and analysis of a four motorized wheels electric vehicle, *International Journal of Vehicle Mechanics and Mobility*, 35(3), 163–194, 2010.

[8] C. J. Wiet, *Energy optimization of an in-wheel-motor electric ground vehicle over a given terrain with considerations of various traffic elements*, M.Sc. Dissertation, Department of Mechanical Engineering, The Ohio State University, 2014.

[9] H. S. Hameed, Brushless DC motor controller design using MATLAB applications, *1st International Scientific Conference of Engineering Sciences - 3rd Scientific Conference of Engineering Science*, Diyala, Iraq, 2018, pp. 44–49.

[10] M. S. Gaya, A. Muhammad, R. A. Abdulkadir, S. N. S. Salim, I. S. Madugu, A. Tijjani, L. A. Yusuf, I. D. Umar and M. T. M. Khairi, Enhanced PID vs model predictive control applied to BLDC motor, *IOP Conference Series: Materials Science and Engineering*, 303, 1–7, 2018.

[11] W. N. Fu and S. L. Ho, A quantitative comparative analysis of a novel flux-modulated permanent-magnet motor for low-speed drive, *IEEE Transactions on Magnetics*, 46(1), 127–134, 2010.

[12] P. Liang, F. Chai, Y. Yu and L. Chen, Analytical model of a spoke-type permanent magnet synchronous in-wheel motor with trapezoid magnet accounting for tooth saturation, *IEEE Transactions on Industrial Electronics*, 66(2), 1162–1171, 2019.

[13] S. S. Farinwata and G. Vachtsevanos, Robust stability of fuzzy logic control systems, *Proceedings of 1995 American Control Conference*, Seattle, USA, 1995, pp. 2267–2271.

[14] N. Saed and M. Mirsalim, Mathematical modeling and analysis of dual-stator permanent magnet brushless DC motor, *9th Annual Power Electronics, Drives Systems and Technologies Conference*, Tehran, Iran, 2018, pp. 48–52.

[15] Y. L. Karnavas, A. S. Topalidis and M. Drakaki, Development of a low cost brushless DC motor sensorless controller using dsPIC30F4011, *7th International Conference on Modern Circuits and Systems Technologies*, Thessaloniki, Greece, 2018, pp. 1–4.

[16] M. Ghasemi and X. Song, Powertrain energy management for autonomous hybrid electric vehicles with flexible driveline power demand, *IEEE Transactions on Control Systems Technology*, In press, doi: 10.1109/TCST.2018.2838555

[17] W. J. Rugh, Linear system theory, in *Prentice-Hall Information and System Sciences Series*, 2nd ed, Thomas Kalaith Series Ed. Prentice Hall, 1996, pp. 142–148.

[18] D. Ambühl, O. Sundström, A. Sciarretta and L. Guzzella, Explicit optimal control policy and its practical application for hybrid electric powertrains, *Control Engineering Practice*, 18(12), 1429–1439, 2010.